International Journal of Applied Earth Observation and Geoinformation 43 (2015) 19–31

International Journal of Applied Earth Observation and Geoinformation

journal homepage: www.elsevier.com/locate/jag

Comparative analysis of different retrieval methods for mapping grassland leaf area index using airborne imaging spectroscopy

Clement Atzberger[a,*], Roshanak Darvishzadeh[b], Markus Immitzer[a], Martin Schlerf[c], Andrew Skidmore[b], Guerric le Maire[d]

[a] University of Natural Resources and Life Sciences (BOKU), Institute of Surveying, Remote Sensing and Land Information, Peter Jordan-Strasse 82,1190 Vienna, Austria
[b] Faculty of Geo-Information Science and Earth Observation (ITC), University of Twente, Hengelosestraat 99, P.O. Box 6, 7500 AA Enschede, The Netherlands
[c] Centre de Recherche Public – Gabriel Lippmann, Département Environnement et Agrobiotechnologies, 41, rue du Brill, L-4422 Belvaux, Luxembourg
[d] CIRAD, UMR Eco&Sols, 2 Place Viala, 34060 Montpellier, France

ARTICLE INFO

Article history:
Available online 29 January 2015

Keywords:
Leaf area index
Radiative transfer model
Look-up table
Narrow band vegetation index
Predictive equation
Sample size

ABSTRACT

Fine scale maps of vegetation biophysical variables are useful status indicators for monitoring and managing national parks and endangered habitats. Here, we assess in a comparative way four different retrieval methods for estimating leaf area index (LAI) in grassland: two radiative transfer model (RTM) inversion methods (one based on look-up-tables (LUT) and one based on predictive equations) and two statistical modelling methods (one partly, the other entirely based on *in situ* data). For prediction, spectral data were used that had been acquired over Majella National Park in Italy by the airborne hyperspectral HyMap instrument. To assess the performance of the four investigated models, the normalized root mean squared error (nRMSE) and coefficient of determination (R^2) between estimates and *in situ* LAI measurements are reported ($n = 41$). Using a jackknife approach, we also quantified the accuracy and robustness of empirical models as a function of the size of the available calibration data set. The results of the study demonstrate that the LUT-based RTM inversion yields higher accuracies for LAI estimation ($R^2 = 0.91$, nRMSE = 0.18) as compared to RTM inversions based on predictive equations ($R^2 = 0.79$, nRMSE = 0.38). The two statistical methods yield accuracies similar to the LUT method. However, as expected, the accuracy and robustness of the statistical models decrease when the size of the calibration database is reduced to fewer samples. The results of this study are of interest for the remote sensing community developing improved inversion schemes for spaceborne hyperspectral sensors applicable to different vegetation types. The examples provided in this paper may also serve as illustrations for the drawbacks and advantages of physical and empirical models.

Introduction

Maps of leaf traits and vegetation biophysical characteristics such as leaf area index (LAI) are useful in ecological research and for modelling of surface energy balance, vegetation productivity, water and CO_2 exchange, as well as biodiversity assessment (Pereira et al., 2013; Pu et al., 2003; Turner et al., 1999). Compared to classical multi-spectral instruments, the quality of such maps has been significantly enhanced through hyperspectral remote sensing (Lee et al., 2004; Schaepman et al., 2009).

Although studies quantifying vegetation biophysical parameters using imaging spectroscopy are numerous, relatively few studies deal with grassland canopies. High quality vegetation maps will help managers of National parks to protect these sensitive ecosystems. More research on the usefulness of imaging spectroscopy for vegetation characterisation is also warranted for preparing the remote sensing community for the upcoming (spaceborne) imaging spectrometers such as EnMap (Segl et al., 2010).

Two main approaches are commonly used for estimating vegetation biophysical characteristics from remotely sensed data (Baret and Buis, 2008; Rivera et al., 2014a):

- Statistical approaches.
- Approaches using physically-based radiative transfer models.

* Corresponding author. Tel.: +43 1 47654 5100.
E-mail addresses: clement.atzberger@boku.ac.at (C. Atzberger), r.darvish@utwente.nl (R. Darvishzadeh), markus.immitzer@boku.ac.at (M. Immitzer), schlerf@lippmann.lu (M. Schlerf), a.k.skidmore@utwente.nl (A. Skidmore), guerric.le_maire@cirad.fr (G. le Maire).

http://dx.doi.org/10.1016/j.jag.2015.01.009

In the statistical approach, regression models are developed from *in situ* data to relate the parameter(s) of interest to the spectral data. To minimize topographic, soil background and atmospheric effects most studies involve the use of spectral vegetation indices (*e.g.*, Haboudane et al., 2004; Khanna et al., 2007; Mutanga and Skidmore, 2004; Thenkabail et al., 2000; Yu et al., 2013). Other studies focus on the analysis of the red edge inflection point (Cho and Skidmore, 2009; Darvishzadeh et al., 2009; Haboudane et al., 2008; Horler et al., 1983) or the use of spectral transformations such as band depth analysis (Im and Jensen, 2008; Schlerf et al., 2010). In addition, several studies investigate the usefulness of full spectrum methods such as partial least square regression (PLSR), principal component regression (PCR), Bayesian model averaging or spectral un-mixing approaches (Asner and Martin, 2008; Atzberger, 2010; Hu et al., 2004; Mirzaie et al., 2014; Zhao et al., 2013). Beside these parametric models, non-parametric approaches such as k-NN are also used (Chirici et al., 2008; Corona et al., 2014; McRoberts et al., 2007; Rivera et al., 2014b).

Statistical models have some advantages fostering their widespread use. For example, some of the mentioned statistical models are easy to apply. Also, suitable software is often readily available (Rivera et al., 2014a). It is well known, however, that developed models sometimes lack transferability to other sites with different vegetation, or transferability to other type of image or acquisition conditions (Baret and Guyot, 1991; Vuolo et al., 2013). Another drawback of statistical models is that they require a set of *in situ* data and that their robustness depends on the properties of this data set (*i.e.*, number, quality and representativeness of available reference samples). A systematic investigation of sample size effects would be informative as the collection of ground truth is usually associated with high costs.

To minimize the reliance on *in situ* data, the physical approach involves the use of radiative transfer models (RTM). These models describe the spectral variation of canopy reflectance as a function of viewing and illumination geometry, canopy, leaf and soil background characteristics and are founded on physical principles. RTM, thus, offer an explicit (and physically based) connection between the vegetation biophysical and biochemical properties and the canopy reflectance as measured by a sensor (Houborg et al., 2007). This enables the simultaneous use of all spectral bands acquired by multi- to hyper-spectral sensors and in particular the most sensitive ones. However, for reasonable retrieval performance, RTM usually require the specification of some input parameters (*e.g.*, average leaf angle, soil background reflectance). For structurally heterogeneous vegetation with multiple canopy layers and leaf clumping at different organization levels, canopy reflectance models require additional parameterization often not readily available (Demarez and Gastellu-Etchegorry, 2000). For structurally less complex grass and crop canopies, suitable results were reported using the relatively simple PROSAIL canopy reflectance model – a combination of the models PROSPECT (Jacquemoud and Baret, 1990) and SAIL (Verhoef, 1984) – as reviewed by Jacquemoud et al. (2009).

RTM do not directly yield estimates of the sought vegetation biophysical parameters. Instead, such models need to be inverted using an appropriate inversion strategy (Kimes et al., 2000; Weiss and Baret, 1999). Available methods include iterative optimization methods (Jacquemoud et al., 1995; Le Maire et al., 2011; Richter et al., 2009), look-up-table (LUT) based inversions (Darvishzadeh et al., 2008a; Rivera et al., 2013; Weiss et al., 2000), and neural networks (Bacour et al., 2006; Schlerf and Atzberger, 2006; Verger et al., 2011). Many studies rely on look-up-tables which are relatively easy to implement, and which provide a search across the entire parameter space in a step width solely limited by the available processing power.

To increase the predictive power and robustness of RTM inversions, feature selection approaches are recommended (Baret and Buis, 2008). Published feature selection methods vary in complexity and range from the use of previously identified absorption wavelengths (Darvishzadeh et al., 2008a; Meroni et al., 2004) to more advanced methods based on statistical selection and elimination criteria (Atzberger, 2010; Atzberger et al., 2013; Verger et al., 2011).

To combine the advantages of physical and statistical approaches, Le Maire et al. (2012, 2008),) and Haboudane et al. (2004) amongst others proposed the development of hyperspectral vegetation indices calibrated on RTM-generated synthetic data (*e.g.*, so called predictive equations) for model inversion. No studies evaluating such predictive equations over grasslands are known. Nor are studies evaluating systematically different statistical and physically based approaches over grassland canopies for better understanding their respective advantages and limits.

To address these research gaps, the study presents the results of a comparative assessment of four retrieval methods against *in situ* LAI measurements in Mediterranean grassland:

- Inversion of the PROSAIL radiative transfer model based on LUT.
- Use of predictive equations solely calibrated on PROSAIL generated data.
- Use of predictive equations partly trimmed using available *in situ* (LAI) data.
- Use of narrow-band vegetation indices based solely on available *in situ* (LAI) data.

Mediterranean grasslands are characterized by heterogeneous canopies with a combination of different plant species in varying proportions (Darvishzadeh et al., 2011). This poses challenges for remote sensing applications (Fisher, 1997; Röder et al., 2007). As little is known about heterogeneous (multiple species) grassland canopies (Darvishzadeh et al., 2008b; Vohland and Jarmer, 2008), more research is warranted to better understand the capabilities and limits of different retrieval algorithms. For illustration purpose, the study also addresses the effect of sampling size on the accuracy and robustness of statistical models.

Material

The study focuses on the mapping of LAI in Majella National Park, Italy. To collect the *in situ* LAI data, a field campaign was conducted during the summer of 2005 roughly corresponding to peak vegetation density. Parallel to the measurement campaign, the HyMap sensor was flown providing the corresponding airborne imaging spectrometer data (Darvishzadeh et al., 2011, 2008a). The time of airborne data collection and the field campaign are indicated in Fig. 1 together with average annual growth profiles (NDVI) of major land cover classes in the study region.

Study area

The study site is located in Majella National Park, Italy (latitude 41°50′–42°14′N, longitude 13°50′–14°14′E, Fig. 2). The park covers an area of 74,095 ha. The landscape is composed of bare rock outcrops, shrubby bushes, and patches of grass/herb vegetation. The present study is focused on grassland. The dominant grass and herb species include *Brachypodium genuense, Briza media, Bromus erectus, Festuca* sp., *Helichrysum italicum, Galium verum, Trifolium pratense, Plantago lanceolata, Sanguisorba officinalis* and *Ononis spinosa* (Cho, 2007).

Table 1
Summary statistics of the field measured biophysical variables of 41 grassland sample plots. Four out of the original forty-five plots had to be removed before analysis, as spectral data were unavailable.

Measured variable	Min.	Mean	Max.	SD	Range	Variation coefficient
LAI ($m^2\ m^{-2}$)	0.72	2.87	7.54	1.59	6.8	0.55
Leaf chlorophyll content ($\mu g\ cm^{-2}$)	18.9	28.7	40.9	4.7	22.0	0.16
Number of dominant species[a]	1	2.34	4	0.81	3	0.35

[a] A species was called "dominant" if it occupied at least 20% of the sampling area.

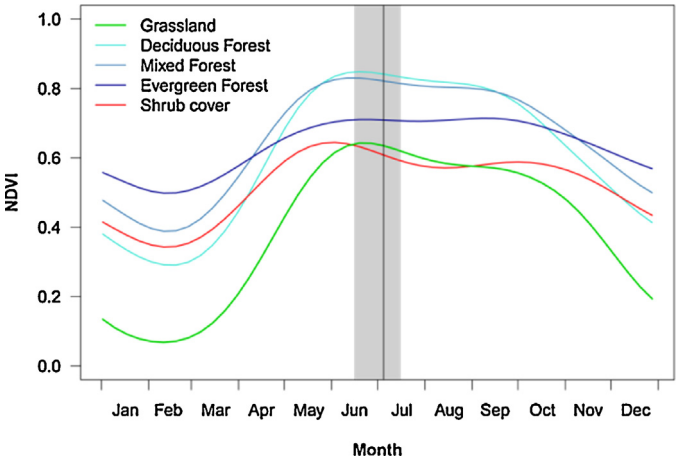

Fig. 1. MODIS NDVI time series (average of 2002–2006) of different land cover types in the region of the study site. The grey area indicates the time period of field work. The vertical black line indicates the acquisition date of the airborne HyMap data cube. Smoothed NDVI data from http://ivfl-info.boku.ac.at/index.php/eo-data-processing.

In situ *measurements*

The field campaign for collecting the *in situ* data was carried out in July 2005 during peak vegetation density (Fig. 1). Vegetation characteristics such as LAI, leaf chlorophyll content and species composition were collected within grassland areas using stratified random sampling and excluding forests, shrublands and bare rock outcrops. Care was taken to ensure sample plots were located at least 500 m (120 pixels) away from strip borders. Strata were derived from a land cover map provided by the management of Majella National Park. Coordinates (x, y) were randomly generated in the grassland stratum to select plots. Forty-five plots of 30 m × 30 m were generated and a GPS was used to locate them in the field. Table 1 summarizes the statistics of the measured variables. For each plot, vegetation parameters were measured *in situ* within four to five randomly selected subplots (1 m × 1 m). From the 4–5 subplots, averages per plot was calculated and used throughout this paper.

LAI was measured non-destructively using the LAI-2000 instrument (Welles and Norman, 1991). The uncertainty of LAI-2000 measurements is typically 15–20% (Chen et al., 1997; Welles and Norman, 1991). Measurements were taken either under overcast conditions or alternatively within two hours after sunrise or before sunset. Direct sunlight on the sensor was prevented using a view restrictor of 45° and shading the sensor. For each subplot, one reference measurement of above-canopy radiation was taken. Next, five below-canopy measurements were performed from which the average subplot LAI was calculated. No corrections for leaf clumping were applied as the necessary information was not available. Likewise, no attempts were made to distinguish between photosynthetic and non/photosynthetic components. This implies that the measurement corresponds strictly speaking to the plant area index (PAI) (Chen et al., 1997). Nevertheless, in the following, these measurements are abbreviated as LAI.

Besides LAI, leaf chlorophyll content was assessed in each 1 m × 1 m subplot. This variable was used for restricting the range of plausible leaf chlorophyll values in the construction of the LUT (see Section "PROSAIL-based LUT generation"). From the dominant grass species, 30 leaves were randomly selected and measured by a SPAD-502 Leaf Chlorophyll Meter (Minolta, 2003). The 30 recorded

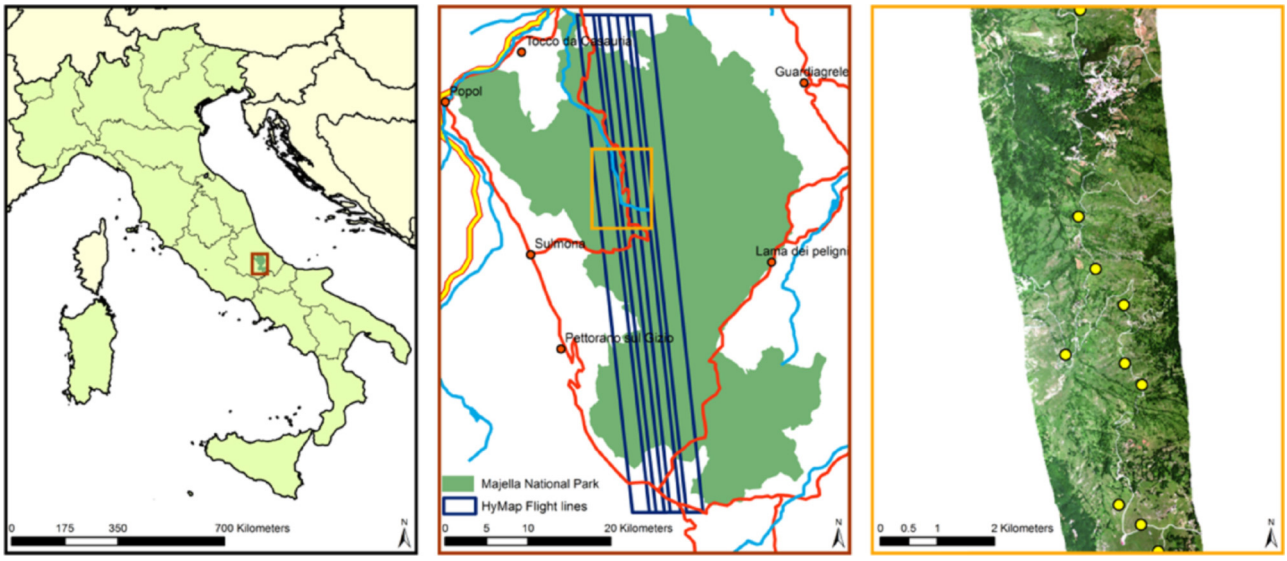

Fig. 2. Location of the study area in Italy (left), map of the Majella National park with flight lines of HyMap (blue) (center) and true colour composite of HyMap image (right) acquired on 4 July 2005 (bands 634, 542 and 452 nm) showing part of the study area (from second image strip). The yellow points indicate the distribution of sample plots in this part of the study area (right).

SPAD readings were averaged. The averaged SPAD readings were converted into leaf chlorophyll contents ($\mu g\,cm^{-2}$) by means of the Markwell et al. (1995) equation. As the Markwell calibration functions were developed for corn and soybean this possibly leads to some bias when applied to grass leaves (Le Maire et al., 2008; Si et al., 2012).

Image acquisition and pre-processing

Airborne HyMap data of the study site were acquired during the field campaign on July 4th, 2005 covering an area of about 40 km × 7 km (four strips with 30% overlap, Fig. 2). The flight was carried out by DLR, Germany's Aerospace Research Centre and Space Agency. The HyMap sensor contains 126 wavelengths, operating over the spectral range of 436–2485 nm. The average spectral resolution is between 13 and 17 nm. At an average flight height of 1983 m above ground, the spatial resolution of the data is 4 m. The image acquisition was close to solar noon and the solar zenith and azimuth angles for the four image strips ranged between 30.0–33.7° and 111.5–121.0°, respectively.

The image strips were atmospherically and geometrically corrected by DLR, Germany. The geometric accuracy of the images was reported by DLR with 2 m (0.5 pixel). The atmospheric correction was performed using ATCOR4-r (rugged terrain). Effects related to the sensor's large field of view were not accounted for, resulting in some visible artefacts towards the borders of the strips. This was deemed acceptable as the sample plots were located mainly in the central parts of the images (Fig. 2).

From the corrected strips, sample plot spectra were retrieved. Owing to cloud coverage in some areas, the spectra of four of the fourty-fiveplots were unreliable and removed. As the pixel size of the imagery was 4 m, a 7 × 7 pixel window (*i.e.*, 28 m × 28 m) centred around the central position of a plot was determined (plot size 30 m × 30 m). By taking only pixels located entirely in the plot, border effects were minimized. From the 7 × 7 pixel window, the average spectrum was calculated. Only these spectra were analysed in this study without any further smoothing or filtering.

Methods

To obtain a comprehensive comparison of LAI retrieval algorithms, this study evaluates four different LAI retrieval methods in a comparative way (Table 2): two RTM inversion methods (one based on look-up-tables, the other based on predictive equations) and two statistical modelling methods (one partly, the other entirely based on *in situ* data). The four methods were chosen because they are the most widely used by the remote sensing community. All procedures were implemented in Matlab (The Mathworks®). Detailed descriptions are given in Sub-sections "Physical based modelling" and "Statistical modelling".

All methods were evaluated against the LAI *in situ* measurements. For the validation of the two PROSAIL inversions (LUT and $PE_{physical}$), the LAI measurements were used as independent observations. The accuracy of the retrievals was characterized by the root mean square error (RMSE) and the coefficient of determination (R^2) between the *in situ* data and the estimates. To evaluate the performance of the two statistical methods ($PE_{re\text{-}adjust}$ and VI), a jackknife sampling procedure was used (see Sub-section "Jackknife sampling"); part of the available *in situ* data was used for model calibration, while the remaining samples were used for independent assessment of the retrieval accuracy. By varying the size of the calibration samples, the effect of sample size on RMSE and R^2 was quantified.

Table 2
Overview of four modelling methods for estimating LAI compared in the present study. The first two methods belong to the category of physical based approaches and the two last methods are statistical approaches making use of *in situ* data for model development. LUT is a standard LUT inversion of radiative transfer models. $PE_{physical}$ and $PE_{re\text{-}adjust}$ are both predictive equations with the difference that the second uses the *in situ* data for fitting the polynomials, whereas the first is entirely calibrated on RTM-generated data. In both cases, the two best wavebands are identified from the RTM-generated data base. VI is similar to $PE_{re\text{-}adjust}$ but entirely calibrated on the experimental (*in situ*) data.

Category	Abbreviation	Wavelengths used	Data base for fitting the polynomials	Use of *in situ* LAI	Description
Physical	LUT	107 Wavelengths[a]	n.a.	Only used for validation	Standard LUT inversion taking the average of the 10 best solutions as final result (includes an image-based feature selection described in Atzberger et al. (2013))
	$PE_{physical}$	$\lambda_1\lambda_2$ from RTM	Simulated from RTM	Only used for validation	The best index-type, wavelengths and polynomials are determined from RTM-generated data base (Le Maire et al., 2008)
Statistical	$PE_{re\text{-}adjust}$	$\lambda_1\lambda_2$ from RTM	Experimental	Cal/Val using jackknife sampling	Best index-type and wavelengths are found from RTM simulations. Polynomials are fitted using *in situ* data
	VI	$\lambda_1\lambda_2$ from experimental data	Experimental	Cal/Val using jackknife sampling	The best index-type, wavelengths and polynomials are determined from experimental (*in situ*) data

[a] The 107 most suitable wavelengths were identified without making use of *in situ* data.

Physical based modelling

The PROSAIL radiative transfer model

The widely used PROSAIL radiative transfer model was selected for the physically based canopy parameter retrieval (Jacquemoud et al., 2009). PROSAIL is relatively simple and needs only a limited number of input parameters. This makes model inversion for retrieval of leaf and canopy parameters feasible.

PROSAIL has been inverted over a large range of vegetation canopies (Darvishzadeh et al., 2011; Jacquemoud et al., 1995; Le Maire et al., 2011; Meroni et al., 2004; Richter et al., 2009, 2011; Si et al., 2012) with varying levels of success. The capacity of PROSAIL to simulate grassland spectra in forward mode was investigated in Darvishzadeh et al. (2008a, 2011),) and in more detail in Atzberger et al. (2013). The general suitability of PROSAIL for grassland studies was also shown by Vohland and Jarmer (2008).

PROSAIL-based LUT generation

Look-up-tables (LUT) provide an easy and robust way for inverting radiative transfer models (Knyazikhin et al., 1999; Weiss et al., 2000). Compared to numerical optimization methods, LUT are much faster and permit a global search (avoiding local minima).

To achieve high accuracy for the estimated parameters, the dimension of the table must be large enough (Combal et al., 2002; Weiss et al., 2000). For our study, a LUT size of 100,000 parameter combinations was chosen. Working with the same RTM, the selected LUT size was found by Weiss et al. (2000) and Richter et al. (2009) to be a good compromise between computation time and the accuracy of the estimates. Following recommendations of Le Maire et al. (2008) the PROSAIL parameter combinations were randomly drawn from uniform distributions and a small white noise component was added to the LUT spectra.

The sensor viewing angle (t_0) and the relative azimuth angle (phi) were fixed at 0° as most plots were in vicinity of the nadir line of the image strips. The sun zenith angle was fixed at 31.5°. With respect to the fraction of diffuse incoming solar radiation (skyl), a fixed value of 0.1 across all wavelengths was used. This simplification seems justified by the fact that skyl has only a very small influence on canopy reflectance (Clevers and Verhoef, 1991).

The eight remaining input parameters of PROSAIL (*i.e.*, LAI, ALA, scale, hot, N, Cab Cm and Cw) were sampled within pre-described ranges. This increases the sampling density in the parameter space and helps to regularize ill-posedness of the inverse problem (Combal et al., 2003). Restricting the parameter space is a recommended procedure used in many similar studies (Verger et al., 2011). The ranges (minimum and maximum) for each of the eight "free" model parameters are reported in Table 3. Note that the ranges of Cab and ALA were selected based on information from field data collection. This implies that the implemented physical approach was not completely independent from field observations.

To represent soil optical properties bare soil pixels were identified within the HyMap scenes. From these pixels spectra were extracted and used to calculate an average soil spectrum (rsl). A multiplicative scale parameter was used to mimic soil brightness changes (Table 4). Concerning the leaf structural parameter N in PROSPECT, we selected a range of 1.5 to 1.9 since grasses have relatively thin leaves. This range was used in a previous study by Darvishzadeh et al. (2008a) and is in agreement with the mean value ($N = 1.6$) that Vohland and Jarmer (2008) used for grassland species. The ranges of the remaining input parameters (Cw, Cm and hot) were similarly selected based on existing literature (Darvishzadeh et al., 2011; Haboudane et al., 2008, 2004; Houborg and Boegh, 2008; Le Maire et al., 2008).

PROSAIL inversion using LUT

To find the solution to the inverse problem, the mean square error (Δ) between measured and modeled (LUT) spectra is calculated for each HyMap spectrum according to:

$$\Delta = \frac{\Sigma_{\lambda=1}^{n}(R_{\text{measured}_\lambda} - R_{\text{lut}_\lambda})^2}{n} \quad (1)$$

where R_{measured} is the measured HyMap reflectance at wavelength λ, R_{lut} is the modeled reflectance at the same wavelength in the LUT, and n is the number of wavebands.

Following recommendations of Combal et al. (2003) and Baret and Buis (2008), the average of the ten parameter sets yielding the lowest Δ is taken as the solution to the inverse problem. For the remainder of this paper, the technique is abbreviated as LUT.

Feature selection using recursive band elimination

A drawback of the physical approach is that corrupted spectral measurements and poorly modeled wavebands negatively affect the model inversion. For this reason, an appropriate band selection is known to improve radiative transfer model inversion (Meroni et al., 2004; Schlerf and Atzberger, 2006). The drawback arises from the fact that RTM inversion uses all the provided spectral information simultaneously. In the case of a LUT-based model inversion, for example, the parameter set is selected as final result, which minimizes the overall error between the simulated and the observed spectra. Hence, any corrupted spectral band will have a negative effect on the selected parameter set as the "solution" is driven into its direction. Similarly, a band which is not well simulated by a RTM receives as much weight as a well simulated wavelength; therefore, deteriorating the inversion results.

Feature selection approaches aim minimizing the negative impacts of poorly modeled wavebands as well as of corrupted spectral data. However, neither the selection of an optimal spectral subset, nor the weighting of spectral bands, are trivial problems but are still open issues within the remote sensing community (Lavergne et al., 2007; Meroni et al., 2004; Rivera et al., 2014b). In Darvishzadeh et al. (2011), the problem of feature selection was addressed by restricting the LUT search to a small number of pre-defined bands that are related to leaf chlorophyll, LAI and leaf dry mass. However, results were not promising. For this reason, in the current paper preference was given to an alternative approach called recursive band elimination (Atzberger et al., 2013; Darvishzadeh et al., 2011). The recursive band elimination technique discards successively wavelengths poorly modeled by PROSAIL. The scene-based approach is fully automatic and does not make use of *in situ* measurements. The reader is referred to the mentioned papers for more details.

PROSAIL inversion using predictive equations

Predictive equations ($\text{PE}_{\text{physical}}$) are investigated in this study as an interesting alternative means to invert the PROSAIL radiative transfer model (Dorigo et al., 2007; Le Maire et al., 2012, 2008; Rivera et al., 2014a). To ensure a perfect comparability, both PROSAIL inversion methods (LUT and $\text{PE}_{\text{physical}}$) use the same LUT.

Using predictive equations, one may identify a suitable narrow band vegetation index and band combination and fit the spectral data against the corresponding vegetation characteristic (here LAI). Three types of common vegetation indices were analyzed for this study: difference index (D), ratio index (R) and normalized difference index (ND). For each index, all possible 126×126 HyMap wavelength combinations between 436 and 2485 nm were systematically calculated:

$$D = \rho_{\lambda 1} - \rho_{\lambda 2} \quad (2a)$$

$$R = \frac{\rho_{\lambda 1}}{\rho_{\lambda 2}} \quad (2b)$$

Table 3
Parameterization of the PROSAIL radiative transfer model for generating the LUT used for model inversion. Parameter values were drawn randomly (uniform distributions) within the specified ranges. For all simulations, the fraction of diffuse incoming radiation (skyl) was fixed at 0.1. The sun zenith angle was fixed at 31.5°. Nadir viewing was assumed. To represent soil optical properties, bare soil pixels were identified within the HyMap scenes. From these pixels spectra were extracted and used to calculate an average soil spectrum (rsl). A multiplicative scale parameter was used to mimic soil brightness changes. Concerning the leaf structural parameter N in PROSPECT we selected a range of 1.5 to 1.9 since grasses have relatively thin leaves. This range was used in a previous study by Darvishzadeh et al. (2008a) and is in agreement with the mean value (N = 1.6) that Vohland and Jarmer (2008) used for grassland species. The ranges of the remaining input parameters (Cw, Cm and hot) were similarly selected based on existing literature (Darvishzadeh et al., 2011; Haboudane et al., 2008, 2004; Houborg and Boegh, 2008; Le Maire et al., 2008).

Parameter	Abbreviation in model	Unit	Minimum value	Maximum value
Leaf area index[a]	LAI	$m^2\ m^{-2}$	0	8
Mean leaf inclination angle[a]	ALA	deg	40	70
Leaf chlorophyll content[a]	C_{ab}	$\mu g\ cm^{-2}$	15	45
Leaf structural parameter	N	No dimension	1.5	1.9
Dry matter content	C_m	$g\ cm^{-2}$	0.005	0.010
Equivalent water thickness	C_w	cm	0.01	0.02
Hot spot size	hot	$m\ m^{-1}$	0.05	0.10
Soil brightness	scale	No dimension	0.5	1.5

[a] Field measurements were consulted to select appropriate minimum and maximum values.

$$NDVI = \frac{\rho_{\lambda 1} - \rho_{\lambda 2}}{\rho_{\lambda 1} + \rho_{\lambda 2}} \quad (2c)$$

where $\rho_{\lambda 1}$ is the reflectance at wavelength $\lambda 1$, and $\rho_{\lambda 2}$ is the reflectance at wavelength $\lambda 2$ with $\lambda 1 \neq \lambda 2$.

For each wavelength combination, a second order polynomial was fit between the index values and the corresponding LAI in the synthetic data base ($n = 100{,}000$). With the fitted polynomial, the LAI was estimated from the HyMap spectra and the RMSE calculated between the estimated and the field measured LAI ($n = 41$) for all possible band combinations. For a given index type, the lowest RMSE in the 2-D plot corresponds to the "best" combination of wavelengths. Because the *in situ* data was not used for model calibration, the field measurements can be considered as independent observations, very similar to the LUT approach. Note that the same set of wavelengths is used in the statistical version of the predictive equation (Section "Statistical modelling") called $PE_{re\text{-}adjust}$ (Table 2).

Statistical modelling

Two statistical modelling methods were tested for comparison with the two physically based methods. Both methods relate 2-band vegetation indices to LAI using 2nd order polynomial fits. The first statistical approach ($PE_{re\text{-}adjust}$) uses the "best" wavelength combination and index-type found in the $PE_{physical}$ approach (Section "PROSAIL inversion using predictive equations"). In contrast, the second statistical technique (VI) finds the best wavelength combination (and index-type) using the *in situ* data. The main difference compared to $PE_{physical}$ is that the polynomials are fitted against the *in situ* data and not against synthetic data. This implies that the *in situ* data is used for calibration and validation issues (Table 2). To ensure comparability with the physical based methods which are no making use of *in situ* data for model calibration, the accuracy of the statistical methods had to be assessed from independent samples. This was achieved using a classical leave-one-out jackknife approach.

Jackknife sampling

To assess the robustness of the two statistical models to calibration sample and sample size, jackknife procedures (without replacement) were used (Table 4). Stratified sampling was used to make sure that the calibration data covers the entire range of LAI values ($0 < LAI < 7$). For this purpose the full data set was split in five equal parts, each with 8–9 observations. Calibration samples (VI: 20; $PE_{re\text{-}adjust}$: 5–35) were drawn making sure that at least one observation was found in all five LAI-classes. Polynomials were only fitted to these balanced samples.

In the case of the VI modelling, the "best" wavelength set is not known beforehand. Each time new random samples is selected for model calibration, all wavelength combinations are scanned within the training data set. The "best" performing set of wavelength (combination of "optimum" wavelengths) is then applied to the left-out samples and the RMSE is determined. Hence, "best" wavelengths may change from iteration to iteration in the case of VI modelling. The whole process was repeated 20,000 times ensuring stability of the results. For practical reasons, only one sample size of twenty samples was assessed. Model accuracy (RMSE, 5% and 95% percentiles) was always calculated from the (twenty-one) left-out samples. For each repetition, the best wavelength combination was stored to assess the robustness of its determination.

A slightly different approach was adopted for $PE_{re\text{-}adjust}$, where the best set of wavelengths is found through analysis of the synthetic data obtained from RTM simulations (Section "PROSAIL inversion using predictive equations"). Hence, this wavelength set will not change during the jackknife sampling. The focus for this method was, therefore, on the sample size. The jackknife sampling was repeated 500,000 times for each sample size between 5 and 35 samples. The corresponding RMSE was calculated between the observed and the estimated (left-out) LAI samples. From the 500,000 repetitions, the median RMSE and the 5% and 95% percentiles were derived for all sample sizes between 5 and 35 samples. The selected number of repetitions ensures stability of the results.

Results

LAI from LUT inversion of PROSAIL

The PROSAIL radiative transfer model was inverted (LUT) for the entire study area covered by the HyMap imagery. From the field plot locations, the forty-one modeled grassland LAI values were extracted and compared to the *in situ* measurements. A scatterplot between the measured and estimated LAI is shown in Fig. 3 (left). The R^2 and the (normalized) RMSE between the measured and estimated LAI are listed in Table 5 (first line).

The comparison between observed and modeled LAI shows that – after feature selection and using the multiple LUT solutions – LAI was estimated with an accuracy of $0.53\ m^2\ m^{-2}$, representing 18% of the average field measured LAI (nRMSE), respectively, 8% of the range of field measured LAI ($0.7 \leq LAI \leq 7.5$). In total, 91% of the observed variance in LAI was explained using this approach.

The LAI map obtained from the LUT-based RTM inversion is presented in Fig. 4. Pixels not corresponding to grassland strata were left blank. The mean LAI obtained for all grassland pixels was

Table 4
Set-up of the jackknife experiments to evaluate the robustness of the two statistical methods ($PE_{re\text{-}adjust}$ and VI) to calibration sample. The focus of $PE_{re\text{-}adjust}$ is on sample size. The focus of VI is on the robustness of the selected "best" wavelengths.

	$PE_{re\text{-}adjust}$	VI
Type of vegetation index (n_{VI})	Only one found « optimum » from RTM-generated data base	Three types of vegetation index (Eq. 3a–3c)
Wavelength combinations (n_W)	Only one found « optimum » from RTM-generated data base	All 126 × 126 possible wavelength combinations
Calibration sample size (n_{SS})	Sample sizes between 3 and 25 samples (all balanced)	Fixed samples size of 20 (all balanced)
Repetitions per case (n_R)	500,000 Random repetitions per case	20,000 Random repetitions per case
Total number of simulations ($n_{VI} \times n_W \times n_{SS} \times n_R$)	1 × 1 × 23 × 500,000	3 × (126 × 126) × 20 × 20,000

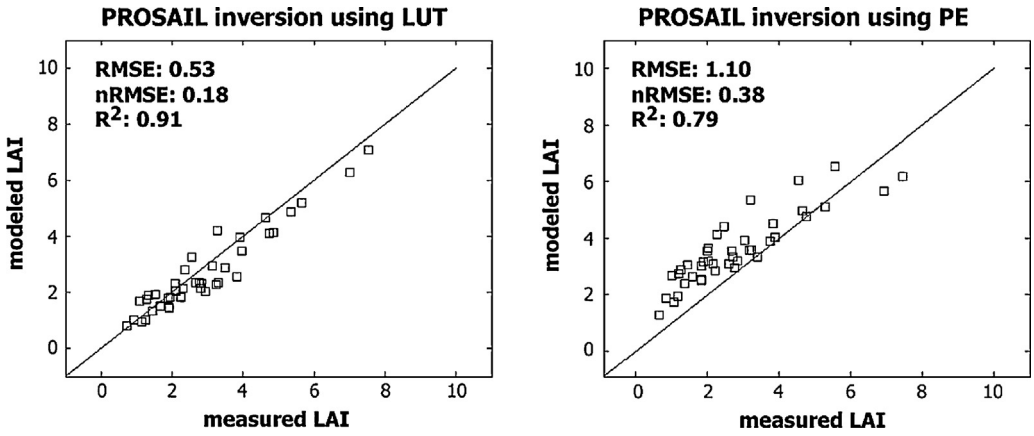

Fig. 3. Estimated versus measured LAI in Majella National Park using the PROSAIL canopy reflectance model with airborne HyMap spectra ($n = 41$). (left) RTM inversion using the standard LUT approach (107 wavelengths and multiple solutions). (right) RTM inversion using predictive equations ($PE_{physical}$) and the *D*-index (λ1: 846 nm, λ2: 1698 nm).

2.9 $m^2\ m^{-2}$, which approximates an average of 2.8 $m^2\ m^{-2}$ that was obtained for the field measurements (Table 2). Most modeled (and observed) LAI were found between 1 and 4 $m^2\ m^{-2}$ (Fig. 5). In both data sets, we observe only a few cases with very high LAI (>4–5).

Comparison of LUT approach with other methods

The results from the three other methods (see Table 2) are presented in the following Sub-sections. A statistical overview of all four methods is provided in Table 5 together with some information regarding the spectral setting and the employed validation.

RTM inversion using predictive equations ($PE_{physical}$)

From the synthetic (PROSAIL simulated) data set, we found that the *D*-index with wavelengths at 846 and 1698 nm was the best performing index for LAI retrieval. The results were obtained by testing all possible band combinations and the three index types (Eqs. (3a)–(3c)). Using reflectances at the two mentioned wavelengths, the *D*-index gave for the synthetic data set a RMSE of 1.08 LAI. Normalized difference and ratio-type indices gave lower performances with RMSE (synthetic data) of ~1.16 LAI (both using wavelengths 756 and 1698 nm).

Subsequent application of the predictive equation developed for the *D*-type index to the experimental (HyMap) data gave the results shown in Fig. 3 (right). Compared to the LUT-based RTM inversion (Fig. 3, left), the LAI retrievals are less accurate (Table 5, second row). The RMSE doubled from 0.53 (LUT_{RTM}) to 1.10 $m^2\ m^{-2}$ ($PE_{physical}$). The increased RMSE was the result of a strong offset and an (slightly) increased scatter.

Re-adjusting predictive equations against experimental data ($PE_{re\text{-}adjust}$)

In the statistical $PE_{re\text{-}adjust}$ approach, the polynomial describing the relation between vegetation index and LAI is re-adjusted using the experimental data, while keeping the same index and wavelengths as in $PE_{physical}$. Results obtained with this approach are summarized in Table 5 (third row). A scatterplot between measured and modeled LAI is shown in Fig. 6 (left).

Table 5
Statistics (R^2, RMSE and normalized RMSE) obtained between field measured and estimated LAI ($n = 41$) from PROSAIL inversion (LUT) and three other methods using airborne HyMap spectra. For the two physically based methods (LUT and $PE_{physical}$) the validation is done directly against the independent in situ data. For the two experimental methods ($PE_{re\text{-}adjust}$ and VI) two validation results are provided: cross-validated results and (in parentheses) the range (5% and 95% percentiles) from the repetitions of the jackknife sampling with twenty samples (CAL-size: 20).

Method	Spectral setting	Validation	LAI ($m^2\ m^{-2}$)		
			R^2	RMSE	nRMSE
LUT	Simultaneous use of 107 bands for LUT search (multiple LUT solutions)	Validation against independent data	0.91	0.53	0.18
$PE_{physical}$	Best 2-band VI within 126 × 126 cases from synthetic data base[a]	Validation against independent data	0.79	1.10	0.38
$PE_{re\text{-}adjust}$	Best 2-band combination from $PE_{physical}$ re-adjusted to experimental data[a]	Cross-validation (CAL-size: 20)	0.75(0.70–0.86)	0.46(0.53–0.79)	0.16(0.21–0.39)
VI	Best 2-band VI within 126 × 126 cases from experimental data base[b]	Cross-validation (CAL-size: 20)[c]	0.86(0.75–0.92)	0.59(0.50–0.76)	0.21(0.17–0.26)

[a] From the synthetic data the best index form was found to be the *D*-index with λ1: 846 nm and λ2: 1698 nm (minimum RMSE on simulated dataset: 1.08).
[b] From the experimental data base, it was found that the *R*-index performed best with λ1: 543 nm and λ2: 1953 nm.
[c] For the jackknife simulation, always the same spectral bands were used previously identified from the entire data set: 543 and 1953 nm.

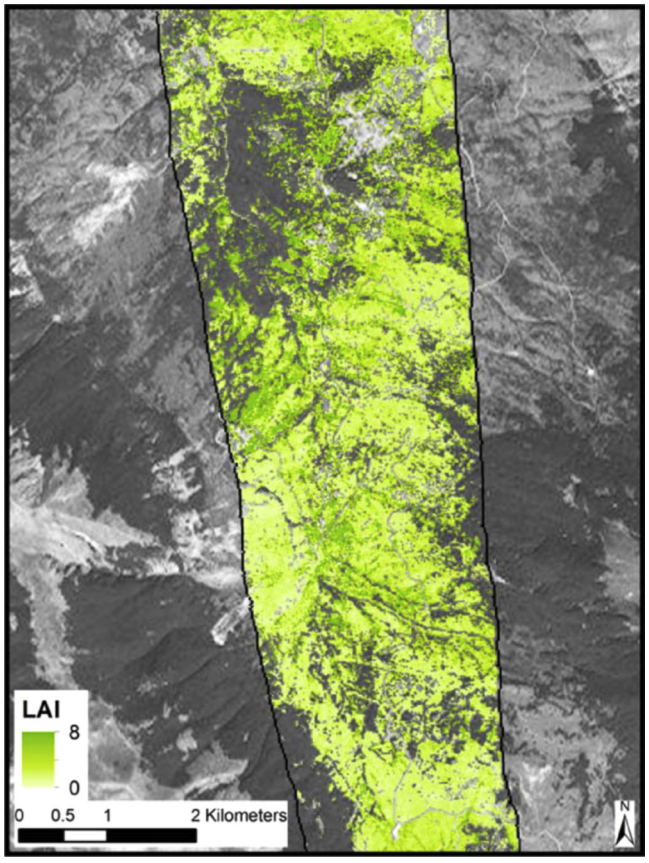

Fig. 4. Map of PROSAIL derived grassland LAI ($m^2\ m^{-2}$) for a subset area of Majella National Park, Italy, using cleaned HyMap data and a LUT-based model inversion solutions. Areas outside the grassland stratum are left transparent. The black lines indicate the extent of the HyMap strip.

Re-adjusting the polynomials against *in situ* data improved the results compared to the PROSAIL inversion based on predictive equations ($PE_{physical}$) (Fig. 3; right). Using the *D*-index with wavelengths optimized on the synthetic data and coefficients fitted to observed data, we obtained a cross-validated RMSE of 0.46 (R^2_{cv}: 0.75). Hence, using the *in situ* data for calibration issues, the accuracy of the standard LUT inversion could be reached. Compared to LUT, the RMSE of $PE_{re\text{-}adjust}$ was (slightly) lower while the R^2 indicated a reduced precision (0.75 against 0.91). In particular, LAI values >4 seem to be estimated with a higher explained variance using LUT (Fig. 3; left) compared to $PE_{re\text{-}adjust}$ (Fig. 6; left).

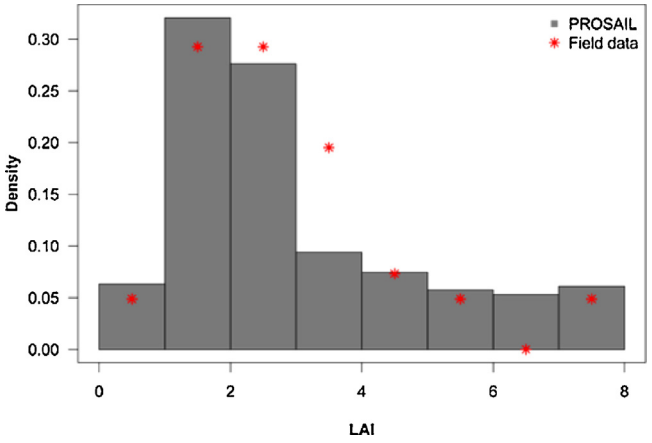

Fig. 5. Observed (dots) and modelled (bars) frequency distribution of LAI. The bars indicate the frequency distribution of PROSAIL derived LAI ($m^2\ m^{-2}$) for a subset area of Majella National Park, Italy, using cleaned HyMap data and a LUT-based model inversion solutions. The dots indicate the distribution of field measurements.

Table 5 (third row in parentheses) gives the expected accuracy range of $PE_{re\text{-}adjust}$ if the calibration size were only twenty samples. As expected, a higher RMSE is observed (RMSE between 0.53 and 0.79 for $PE_{re\text{-}adjust}$ compared to 0.53 for LUT). This highlights the impact of sample size when dealing with statistical approaches even if the samples were well balanced from low to high values as in this study. A more detailed assessment of this issue is presented in Section "Impact of sample and sample size on PEre-adjust and VI".

Optimization of vegetation indices against experimental data (VI)

In the second statistical approach (VI method), narrow band *D*-, ND- and *R*-like indices were calculated from the HyMap reflectance spectra. The *in situ* LAI data were sequentially regressed (polynomials) against all possible (126×126) two-band combinations of each index type. This allowed us to determine and fix the optimum wavelength combination for each index.

With the optimum wavelength combination, LAI was estimated in cross-validation mode. The optimum indices of the three index types gave similar results for estimating LAI ($RMSE_{cv}$ between 0.59 and 0.62; R^2_{cv} between 0.85 and 0.86). The *R*-index using wavelengths at 543 and 1953 nm had a higher R^2 compared to *D*- and ND-like indices. The statistics of this index are summarized in Table 5 (last row) together with the three other methods. A scatterplot of measured and cross-validated LAI is shown in Fig. 6 (right).

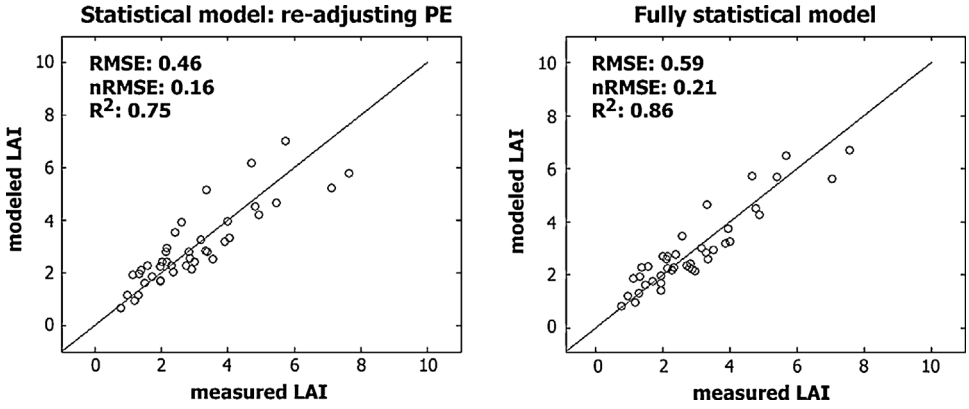

Fig. 6. Measured versus estimated (cross-validated) LAI in Majella National Park using statistical approaches with airborne HyMap spectra ($n = 41$). (left) Re-adjusting the polynomials against in situ data ($PE_{re\text{-}adjust}$): *D*-index with (λ1: 846 nm, λ2: 1698 nm. (right) Identification of optimum index form, wavelengths and polynomials from experimental data (VI): *R*-index (λ1: 543 nm, λ2: 1953 nm).

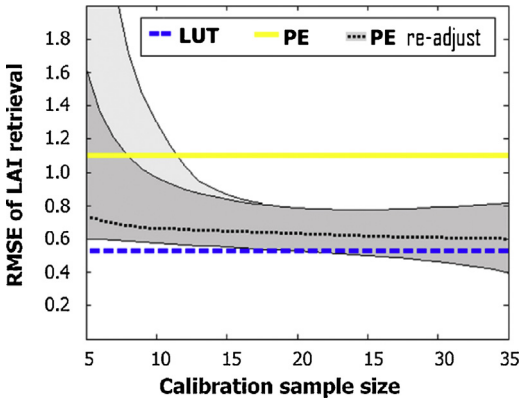

Fig. 7. Accuracy (RMSE) of grassland LAI retrieval using different modelling-methods. Results of the two physically based methodsare shown in blue (LUT), respectively, in yellow ($PE_{physical}$). As no calibration step was involved for inverting the RTMs, the reported RMSE do not depend on the calibration sample size. For the statistical model $PE_{re\text{-}adjust}$ (black dotted line), results obtained with the *D*-index (with λ1: 846 nm and λ2: 1698 nm) are shown. For each calibration sample size (between 5 and 35 samples) 500,000 replicates were randomly selected and used to predict the left-out samples. The shaded dark gray area indicates the 5– 95% percentiles of the statistical model when stratified sampling was used. In light gray are shown the results when sampling was completely random. (For interpretation of the references to colour in this figure legend, the reader is referred to the web version of this article.)

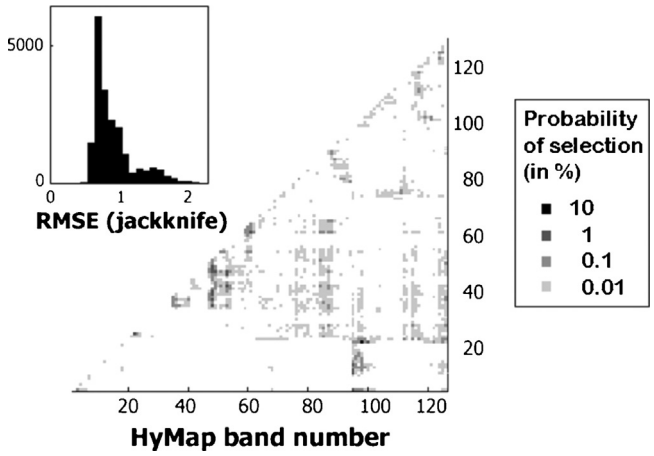

Fig. 8. Results of the jackknife sampling (VI method) with twenty randomly selected calibration samples and the *R*-index. The 2-dimensional plot shows the probability of a 2-band combination being selected. To ease interpretations, the results were recoded in four log 10-spaced classes. For the calculations 20,000 random iterations were run each testing all 126 × 126 band combinations. The inlet shows the frequency distribution of the RMSE for the 20,000 validation samples (each calculated over twenty-one left-out LAI observations and for the best band combination).

The VI method yielded comparative results with RMSE as low as for LUT and $PE_{re\text{-}adjust}$.

Again, a strong impact of sample size has to be mentioned. Compared to the cross-validated results – which gave a RMSE of 0.59 m^2 m^{-2} – the jackknife sampling with twenty calibration samples resulted in a RMSE between 0.50 and 0.76 m^2 m^{-2}. However, this estimate is overoptimistic. Indeed, in practice, one does not know beforehand the "optimum" wavelength combination. In the present case, the jackknife sampling was run keeping the waveband combination from the leave-one-out approach. This issue will be further developed in the next Sub-section.

Impact of sample and sample size on $PE_{re\text{-}adjust}$ and VI

The impact of sampling was further quantified for the two statistical methods ($PE_{re\text{-}adjust}$ and VI). The developed jackknife sampling (see Table 4 for details) tries to mimic in a realistic way what would happen (in terms of accuracy and model robustness) if few(er) samples would be available for model calibration (*e.g.*, only twenty samples).

Sampling effects on $PE_{re\text{-}adjust}$

The variability of the LAI retrieval error (RMSE) as a function of the size of the calibration sample is illustrated in Fig. 7 (in gray) for the *D*-index ($D_{846/1698}$). Whereas in Table 5 (third row in parentheses), only the range of RMSE for a sample size of twenty samples was indicated (*e.g.*, 0.53–0.79), here all values for sample sizes between 5 and 35 samples are graphically shown. As expected, with decreasing sample size the average (median) error shows a steady increase (dashed black line). At the same time, the variability in the RMSE strongly increases, both for the stratified sampling to cover the observed LAI range (in dark gray) and (even more pronounced) for the un-stratified sampling (in light gray). Note that these variabilities are observed despite the fact that the two wavelengths entering the *D*-index were fixed.

Sampling effects on VI_{EXP}

Using the purely statistical approach (VI), the "optimum" wavelength set is not known beforehand but is found from the calibration data. While doing the (stratified) jackknife sampling, the "optimum" wavelengths may, therefore, change from iteration to iteration adding uncertainty to the retrievals.

To remedy this issue, the jackknife approach was run using the *R*-index with twenty calibration samples (20,000 replicates). At each iteration, the optimum wavelength combination was stored as well as the corresponding RMSE (LAI) obtained over the remaining twenty-one left-out samples of the experimental data base. The number of times a given wavelength combination was selected during 20,000 replicates is shown in Fig. 8. The inlet in Fig. 8 shows the resulting frequency distribution of the RMSE.

The figure demonstrates that using twenty calibration samples (even if balanced), the "optimum" waveband combination may be located in quite different parts of the 2-dimensional feature space. Amongst the possible (15,750) two-band combinations, 1068 were at least selected once. The top 20 (top 200) two-band combinations account for 48.5% (87.2%) of the cases. Hence, not only the polynomials are subject to variation but also the "optimum" wavelengths. The fact that the wavelength positions are to be determined from the calibration sample in a purely statistical (VI) approach was not considered in Table 5 (last row). In Table 5, only the RMSE range (5–95% percentiles) for a fixed (optimum) wavelength combination was reported. Our examples demonstrate that in reality one should expect larger errors than those reported in Table 5, in particular for smaller sample size (*e.g.*, the RMSE distribution shown in the inlet of Fig. 8 for a sample size of twenty).

Despite this wide scatter in optimum wavelength combinations, two broad regions appear in Fig. 8 with a higher density of selected cases. The areas depict a broad region between 900 and 1400 nm and another one combining visible wavelengths (550 nm) with SWIR bands (1950 nm). These are spectral regions generally well suited for statistical modelling (Le Maire et al., 2008; Rivera et al., 2014a).

Discussion

Inversion of the PROSAIL radiative transfer model yielded RMSE values between *in situ* and modeled LAI of 0.53 m^2 m^{-2} (Table 5 and Fig. 5). This finding supports previous studies, which demonstrated that inversion of a radiative transfer model may yield accuracies comparable to those of statistical approaches (Atzberger et al., 2010; Gemmell et al., 2002; Le Maire et al., 2012, 2011). The modelling results have been obtained despite the fact that the field

Table 6
Summary of advantages and drawbacks of four LAI retrieval methods.

Method	Advantages	Drawbacks
LUT	• No model calibration is required • Takes into account the full set of spectral bands and is therefore relatively insensitive to random noise • Good accuracy and precision, for the full range of LAI • Generic: applicable for different images, dates, acquisition geometries, *etc.*; in principle even data from different sensors can be combined	• Requires a RTM well suited for the studied vegetation type; suitable RTMs are not equally available for all types of vegetation (*e.g.,* forests) • Needs computing skills, and some computational resources to apply it (in particular if large areas are to be processed) • Requires information for model parameterization (*i.e.* the appropriate range of important model parameters)
$PE_{Physical}$	• After calibration, model inversion is extremely fast and simple • Makes (partially) use of physical knowledge incorporated in the RTM	• Same drawbacks as for LUT • May select unreliable wavelength combinations due to problems with simulated and/or measured data • Precision on LAI retrieval may suffer from offset and noise in the spectral data • Information available in additional wavebands is neglected
$PE_{re\text{-}adjust}$	• Simple to apply • Semi-empirical technique combining some advantages of physical and statistical approaches • Relatively insensitive to additive or multiplicative spectral errors (depending on VI type)	• Requires a well-chosen data set for model calibration (i.e., must be representative for all potential conditions, not only LAI) • Information available in additional wavebands is neglected
VI	• Often yields locally very accurate results with minimum modelling efforts • Simple modelling/calibration technique which can be quickly applied to larger images • Can be used to map all kind of vegetation parameters not necessarily being part of existing radiative transfer models	• Requires a well-chosen data set for model calibration (i.e., must be representative for all potential conditions, not only LAI) • Lacks sometimes generalization and reproducibility and therefore impeding transfer to other images or conditions • Information available in additional wavebands is neglected

measured (*in situ*) data from the LAI-2000 instrument correspond strictly speaking to plant area index (PAI) and not LAI. It also confirms the general validity of PROSAIL for grassland studies as shown in Vohland and Jarmer (2008) and Atzberger et al. (2013).

In our study, a combination of scene-based feature selection (*i.e.*, recursive band elimination) and the use of multiple LUT solutions was used for RTM inversion (Table 2), and it was demonstrated that this inversion approach yields good results. Other inversion schemes were not tested.

One of the benefits of using physical rather than statistical methods is that comprehensive field measurements are not required for model calibration. Using physical methods, field measured LAI are only needed for proper validation. In addition, developed RTMs can in principle be directly applied to other images, with different band settings and/or measurement geometries, *etc.* (Darvishzadeh et al., 2011). Although statistical models have been developed and successfully applied across time and space, this is not always possible.

Drawbacks of physical approaches relate to the fact that results are sometimes not consistent especially where one deals with multiple species in semi-natural environments. The inversion of physically based models is also hampered by the ill-posed inverse problem (Combal et al., 2002; Meroni et al., 2004). In the current work, this problem was alleviated by using multiple solutions in a LUT approach. This reduces the problems obtained when focusing only on the best fitting spectra as final solution. In addition, parameter ranges in the LUT were restricted according to available field measurements (Table 2). Several alternative approaches exist for further regularizing the inverse problem but were not considered in this study (Baret and Buis, 2008): (i) approaches using statistical models for deriving *a priori* information for RTM inversion (Houborg et al., 2007), (ii) approaches using spatial (color texture) features in the RTM inversion in addition to classical spectral-directional signatures (Atzberger and Richter, 2012), (iii) approaches based on the inversion of multi-temporal patch ensembles (Koetz et al., 2005; Lauvernet et al., 2008), and (iv) boot-strap methods for making use of the reflectance uncertainty matrix in the cost function (Lavergne et al., 2007).

The imposed upper/lower boundaries in the LUT had a logical consequence that parameters reached the bounds (not shown). This contradicts somewhat the physical approach as the prior information may have a stronger effect on the retrieved canopy parameters compared to the observed signature (Baret and Buis, 2008). On the other hand, this is what one expects in the case of an ill-posed inverse problem, which may lead to solutions far away from the "true" parameter combination. Alternative ways of imposing expected parameter values in the search function exist but were not further exploited (*e.g.*, Combal et al., 2002; Haboudane et al., 2008; Houborg and Boegh, 2008; Jacquemoud et al., 2009). For example, it is possible to specify in the cost function the expected value of each parameter together with its associated uncertainty. This yields a smooth(er) influence of the *a priori* information on the retrieved parameters. As the aim of the present study was to use a minimum of available *in situ* information, we restricted ourselves to specifying only lower and upper boundaries of the PROSAIL parameters.

In addition to the aforementioned problems, one should note that relatively simple RTM such as the PROSAIL model are not equally applicable to all vegetation types. Canopies such as forests with strong leaf clumping at several scales and with (depth) gradients are more challenging compared to (structurally) still relatively simple grass canopies (Gemmell et al., 2002; Lee et al., 2004; Yang et al., 2011). For the Mediterranean grasslands in the Majella National Park, it was verified in another paper (Atzberger et al., 2013) that the PROSAIL model yields spectral signatures close to the HyMap measurements when model parameters were specified according to field observations. This fully justifies its use within the current study.

The results of our study do not favor the use of predictive equations ($PE_{physical}$) entirely calibrated on synthetic (RTM-generated) data bases (Table 5). In our study, this approach yielded models with significantly lower accuracies as compared to the LUT-based inversion (RMSE of 1.10 as compared to 0.53 $m^2\,m^{-2}$) probably because the selected wavebands (846 and 1698 nm) were not well simulated by the model. For example, in another study, PROSAIL simulated reflectances at these two wavelengths, did not match well observed HyMap reflectances (Atzberger et al., 2013). The reasons for the observed disagreement are not fully clear but are probably related to the absorption coefficients used in the PROSPECT model. Hence, although $PE_{physical}$ selected two wavebands which were generally well suited for LAI modelling, the (polynomial) regression coefficients calibrated using the synthetic data yielded a significant bias in the modeled LAI. Additional problems may arise from the fact that for generating the synthetic data

base, possible cross-correlations between model parameters were not considered. Instead, the parameter distributions were drawn independently from each other. The problem can be circumvented by using experimental data for re-adjusting the polynomials while keeping the previously identified wavelengths (Le Maire et al., 2008). Using this $PE_{re\text{-}adjust}$ approach, the study demonstrated accurate retrievals. The cross-validated RMSE (0.46 m^2 m^{-2}) was as low as the one using the LUT approach, with however a somewhat reduced R^2 (0.75 instead of 0.91) (Table 5).

The (semi-empirical) $PE_{re\text{-}adjust}$ approach has the advantage that it keeps the robustness of the index choice because of its identification within a (large) synthetic dataset. This should result in more generic results, whereas the model fine-tuning is done on the experimental data yielding (locally) highly accurate results.

Regarding the VI approach, LAI was retrieved with high accuracy. The selected wavelength at 1953 nm is sensitive to LAI and leaf water content. This spectral region was found useful in a number of studies even when other vegetation types or sensors were studied (Darvishzadeh et al., 2008a,b, 2009, 2011; Le Maire et al., 2008). In particular, there is good evidence from physical as well as empirical studies that this so-called 'water feature' is sensitive to LAI as the total leaf area is highly correlated with the canopy water content (as plants aim maintaining a relatively constant leaf water content). Similar findings were obtained in forests (Schlerf et al., 2005) where the "best" hyperspectral VI (in relation to LAI) were typically based on wavebands related to prominent water absorption features.

An important drawback of methods such as $PE_{re\text{-}adjust}$ and VI relates to the reproducibility and stability of the fitted models. A strong impact of sampling and sample size was demonstrated in Fig. 7 for the $PE_{re\text{-}adjust}$ method. Indeed, a relatively small calibration sample (*e.g.*, twenty samples) may yield excellent results in one case, but may yield up to 50% higher RMSE in another case; and this despite the fact that sampling was made in a stratified (balanced) manner. For VI this problem is further amplified as the optimum waveband combination is also determined from the experimental data. We have shown (Fig. 8) that for a sample size of twenty calibration samples, the selected "best" band combination lacks robustness.

Summary and conclusions

In our communication, we have demonstrated advantages and drawbacks of four widely used statistical and physical modelling approaches. The key differences between the different modelling methods are summarized in Table 6. The table aims informing practitioners and researchers to identify the most suitable approach for their study. The table also highlights key research questions. As any study that makes reference to a particular data set, our findings are necessarily restricted. Nevertheless, we believe that our key findings are of general validity.

The study has demonstrated that radiative transfer models and hyperspectral airborne imaging can be successfully linked for mapping and assessing leaf area index in Mediterranean grasslands (nRMSE = 0.18; R^2 = 0.91). The employed inversion procedure and recursive band elimination scheme are of interest for the remote sensing community working in different spectral regions and vegetation types. With the launch of spaceborne hyperspectral sensors such as EnMap the availability of suitable data sets will increase. Hence, the application of the developed methods to other vegetation types can be evaluated for assessing their robustness for mapping important vegetation biophysical properties.

The study also demonstrated that grassland LAI can be estimated through the inversion of the PROSAIL radiative transfer model with accuracies comparable to statistical approaches based on vegetation indices. Although still necessary, ground-measured biophysical data may be almost entirely used for validating the retrieved model parameters. Field measurements are not required for model calibration. In our study, *in situ* data were only used for restricting the range of parameters in the look-up-tables (LUT). Additionally, soil optical properties had to be specified according to local conditions. This information is, however, readily obtained from the imagery itself.

The use of radiative transfer models for vegetation biophysical parameter retrieval is sometimes described as something overly complicated. We do not believe that this is really the case. For example, in our study, model inversion was done using LUT. These can be built easily for all kinds of RTM. Also it is quite easy to find within a LUT the simulated spectrum closest to the spectrum being inverted – and thus the solution to the inverse problem. Nonetheless, such approaches are of course still more complicated compared to the calibration and application of LAI-VI models.

In our view, the main drawback of RTM relates to the availability of suitable radiative transfer models for the studied ecosystem and the need to atmospherically correct the remotely sensed imagery. Suitable RTM are not equally available for all types of vegetation (*e.g.*, forests with multiple canopy layers, row crops). Also, the chosen RTM may not incorporate the particular biophysical parameter a researcher might be interested in. For example, adding absorption coefficients of polyphenols (tannin) into PROSPECT for studying tea quality (Bian, 2013) was only partly successful.

One key research question coming out of this study relates to the use (or not) of the full spectral resolution provided by imaging spectrometers. Indeed, one important difference between radiative transfer models and the other methods relates to the number of spectral bands used for LAI retrieval. Whereas the physical modelling approach considers the entire spectral shape in each pixel, the other three methods rely only on two spectral bands (albeit selected from the entire band set). This has implications in terms of computer resources but also noise sensitivity, robustness, generalization and reproducibility. Although generally it might be preferable to make use of the full spectral resolution, our study demonstrated that even with two spectral bands one may (locally) obtain very good results. Hence, it still has to be proven that the detailed spectral shape of a pixel contains information going beyond that of narrow band vegetation indices. On the other hand, if only two spectral bands are to be used, our study showed a clear advantage of using the $PE_{Re\text{-}adjust}$ method which combines some advantages of physical and statistical approaches.

Acknowledgements

We would like to acknowledge the assistance of the park management of Majella National Park, Italy, and in particular of Teodoro Andrisano. Special thanks go to Fabio Corsi, Moses Cho and Istiak Sobhan for their assistance during the field campaign.

References

Asner, G.P., Martin, R.E., 2008. Spectral and chemical analysis of tropical forests: scaling from leaf to canopy levels. Remote Sens. Environ. 112, 3958–3970, http://dx.doi.org/10.1016/j.rse.2008.07.003

Atzberger, C., 2010. Inverting the PROSAIL canopy reflectance model using neural nets trained on streamlined databases. J. Spectral Imaging 1, 1–13, http://dx.doi.org/10.1255/jsi.2010 a2

Atzberger, C., Darvishzadeh, R., Schlerf, M., Le Maire, G., 2013. Suitability and adaptation of PROSAIL radiative transfer model for hyperspectral grassland studies. Remote Sens. Lett. 4, 55–64, http://dx.doi.org/10.1080/2150704X2012.689115

Atzberger, C., Guérif, M., Baret, F., Werner, W., 2010. Comparative analysis of three chemometric techniques for the spectroradiometric assessment of canopy chlorophyll content in winter wheat. Comput. Electron. Agric. 73, 165–173, http://dx.doi.org/10.1016/j.compag.2010.05.006

Atzberger, C., Richter, K., 2012. Spatially constrained inversion of radiative transfer models for improved LAI mapping from future sentinel-2 imagery. Remote Sens. Environ. 120, 208–218, http://dx.doi.org/10.1016/j.rse.2011.10.035

Bacour, C., Baret, F., Béal, D., Weiss, M., Pavageau, K., 2006. Neural network estimation of LAI, fAPAR, fCover and LAI × Cab from top of canopy MERIS reflectance data: principles and validation. Remote Sens. Environ. 105, 313–325, http://dx.doi.org/10.1016/j.rse.2006.07.014

Baret, F., Buis, S., 2008. Estimating canopy characteristics from remote sensing observations: review of methods and associated problems. In: Liang, S. (Ed.), Advances in Land Remote Sensing. Springer, Netherlands, pp. 173–201.

Baret, F., Guyot, G., 1991. Potentials and limits of vegetation indices for LAI and APAR assessment. Remote Sens. Environ. 35, 161–173, http://dx.doi.org/10.1016/0034-4257(91)90009-U

Bian, M., 2013. Assessing the quality of tea by hyperspectral techniques (Ph.D. Thesis). University of Twente Faculty of Geo-Information and Earth Observation (ITC), Twente (NL).

Chen, J.M., Rich, P.M., Gower, S.T., Norman, J.M., Plummer, S., 1997. Leaf area index of boreal forests: theory, techniques, and measurements. J. Geophys. Res. Atmos. 102 (29), 429–29443, http://dx.doi.org/10.1029/97JD01107

Chirici, G., Barbati, A., Corona, P., Marchetti, M., Travaglini, D., Maselli, F., Bertini, R., 2008. Non-parametric and parametric methods using satellite images for estimating growing stock volume in alpine and Mediterranean forest ecosystems. Remote Sens. Environ. 112, 2686–2700, http://dx.doi.org/10.1016/j.rse.2008.01.002

Cho, M.A., 2007. Hyperspectral Remote Sensing of Biochemical and Biophysical Parameters: The Derivative Red-edge Double-peak Feature: A Nuisance or an Opportunity? (Ph.D. Thesis). Wageningen University (NL), Wageningen.

Cho, M.A., Skidmore, A.K., 2009. Hyperspectral predictors for monitoring biomass production in Mediterranean mountain grasslands: Majella National Park, Italy. Int. J. Remote Sens. 30, 499–515, http://dx.doi.org/10.1080/01431160802392596

Clevers, J., Verhoef, W., 1991. Modelling and synergetic use of optical and microwave remote sensing. Report 2: LAI estimation from canopy reflectance and WDVI: A sensitivity analysis with the SAIL model (No. 90–39), BCRS Report.

Combal, B., Baret, F., Weiss, M., 2002. Improving canopy variables estimation from remote sensing data by exploiting ancillary information. Case study on sugar beet canopies. Agronomie 22, 205–215, http://dx.doi.org/10.1051/agro:2002008

Combal, B., Baret, F., Weiss, M., Trubuil, A., Macé, D., Pragnère, A., Myneni, R., Knyazikhin, Y., Wang, L., 2003. Retrieval of canopy biophysical variables from bidirectional reflectance: using prior information to solve the ill-posed inverse problem. Remote Sens. Environ. 84, 1–15, http://dx.doi.org/10.1016/S0034-4257(02)35-4

Corona, P., Fattorini, L., Franceschi, S., Chirici, G., Maselli, F., Secondi, L., 2014. Mapping by spatial predictors exploiting remotely sensed and ground data: a comparative design-based perspective. Remote Sens. Environ. 152, 29–37, http://dx.doi.org/10.1016/j.rse.2014.05.011

Darvishzadeh, R., Atzberger, C., Skidmore, A.K., Abkar, A.A., 2009. Leaf area index derivation from hyperspectral vegetation indicesand the red edge position. Int. J. Remote Sens. 30, 6199–6218, http://dx.doi.org/10.1080/01431160902842342

Darvishzadeh, R., Atzberger, C., Skidmore, A., Schlerf, M., 2011. Mapping grassland leaf area index with airborne hyperspectral imagery: a comparison study of statistical approaches and inversion of radiative transfer models. ISPRS J. Photogramm Remote Sens. 66, 894–906, http://dx.doi.org/10.1016/j.isprsjprs.2011.09.013

Darvishzadeh, R., Skidmore, A., Schlerf, M., Atzberger, C., 2008a. Inversion of a radiative transfer model for estimating vegetation LAI and chlorophyll in a heterogeneous grassland. Remote Sens. Environ. 112, 2592–2604, http://dx.doi.org/10.1016/j.rse.2007.12.003

Darvishzadeh, R., Skidmore, A., Schlerf, M., Atzberger, C., Corsi, F., Cho, M., 2008b. LAI and chlorophyll estimation for a heterogeneous grassland using hyperspectral measurements. ISPRS J. Photogramm Remote Sens. 63, 409–426, http://dx.doi.org/10.1016/j.isprsjprs.2008.01.001

Demarez, V., Gastellu-Etchegorry, J.P., 2000. A modeling approach for studying forest chlorophyll content. Remote Sens. Environ. 71, 226–238, http://dx.doi.org/10.1016/S0034-4257(99)89-9

Dorigo, W.A., Zurita-Milla, R., de Wit, A.J.W., Brazile, J., Singh, R., Schaepman, M.E., 2007. A review on reflective remote sensing and data assimilation techniques for enhanced agroecosystem modeling. Int. J. Appl. Earth Obs. 9, 165–193, http://dx.doi.org/10.1016/j.jag.2006.05.003

Fisher, P., 1997. The pixel: a snare and a delusion. Int. J. Remote Sens. 18, 679–685, http://dx.doi.org/10.1080/014311697219015

Gemmell, F., Varjo, J., Strandstrom, M., Kuusk, A., 2002. Comparison of measured boreal forest characteristics with estimates from TM data and limited ancillary information using reflectance model inversion. Remote Sens. Environ. 81, 365–377, http://dx.doi.org/10.1016/S0034-4257(02)12-3

Haboudane, D., Miller, J.R., Pattey, E., Zarco-Tejada, P.J., Strachan, I.B., 2004. Hyperspectral vegetation indices and novel algorithms for predicting green LAI of crop canopies: modeling and validation in the context of precision agriculture. Remote Sens. Environ. 90, 337–352, http://dx.doi.org/10.1016/j.rse.2003.12.013

Haboudane, D., Tremblay, N., Miller, J.R., Vigneault, P., 2008. Remote estimation of crop chlorophyll content using spectral indices derived from hyperspectral data. IEEE Trans. Geosci. Remote Sens. 46, 423–437, http://dx.doi.org/10.1109/TGRS2007.904836

Horler, D.N.H., Dockray, M., Barber, J., 1983. The red edge of plant leaf reflectance. Int. J. Remote Sens. 4, 273–288, http://dx.doi.org/10.1080/01431168308948546

Houborg, R., Boegh, E., 2008. Mapping leaf chlorophyll and leaf area index using inverse and forward canopy reflectance modeling and SPOT reflectance data. Remote Sens. Environ. 112, 186–202, http://dx.doi.org/10.1016/j.rse.2007.04.012

Houborg, R., Soegaard, H., Boegh, E., 2007. Combining vegetation index and model inversion methods for the extraction of key vegetation biophysical parameters using Terra and Aqua MODIS reflectance data. Remote Sens. Environ. 106, 39–58, http://dx.doi.org/10.1016/j.rse.2006.07.016

Hu, B., Miller, J.R., Chen, J.M., Hollinger, A., 2004. Retrieval of the canopy leaf area index in the BOREAS flux tower sites using linear spectral mixture analysis. Remote Sens. Environ. BOREAS Remote Sens. Sci. 89, 176–188, http://dx.doi.org/10.1016/j.rse.2002.06.003

Im, J., Jensen, J.R., 2008. Hyperspectral remote sensing of vegetation. Geogr. Compass 2, 1943–1961, http://dx.doi.org/10.1111/j1749-8198.2008.00182.x

Jacquemoud, S., Baret, F., 1990. PROSPECT: a model of leaf optical properties spectra. Remote Sens. Environ. 34, 75–91, http://dx.doi.org/10.1016/0034-4257(90)90,100-Z

Jacquemoud, S., Baret, F., Andrieu, B., Danson, F.M., Jaggard, K., 1995. Extraction of vegetation biophysical parameters by inversion of the PROSPECT + SAIL models on sugar beet canopy reflectance data. Application to TM and AVIRIS sensors. Remote Sens. Environ. 52, 163–172, http://dx.doi.org/10.1016/0034-4257(95)00018-V

Jacquemoud, S., Verhoef, W., Baret, F., Bacour, C., Zarco-Tejada, P.J., Asner, G.P., François, C., Ustin, S.L., 2009. PROSPECT + SAIL models: a review of use for vegetation characterization. Remote Sens. Environ., 56–66, http://dx.doi.org/10.1016/j.rse.2008.01.026, Imaging Spectroscopy Special Issue 113, Supplement 1.

Khanna, S., Palacios-Orueta, A., Whiting, M.L., Ustin, S.L., Riaño, D., Litago, J., 2007. Development of angle indexes for soil moisture estimation, dry matter detection and land-cover discrimination. Remote Sens. Environ. 109, 154–165, http://dx.doi.org/10.1016/j.rse.2006.12.018

Kimes, D.S., Knyazikhin, Y., Privette, J.L., Abuelgasim, A.A., Gao, F., 2000. Inversion methods for physically-based models. Remote Sens. Rev. 18, 381–439, http://dx.doi.org/10.1080/02757250009532396

Knyazikhin, Y., Glassy, J., Privette, J.L., Tian, Y., Lotsch, A., Zhang, Y., Wang, Y., Morisette, J.T., Votava, P., Myneni, R.B., Nemani, S.W., Running, S.W., 1999. MODIS Leaf Area Index (LAI) and Fraction of Photosynthetically Active Radiation Absorbed by Vegetation (FPAR) Product (MOD15) Algorithm, Theoretical Basis Document. NASA Goddard Space Flight Center, Greenbelt, MD 20771, USA.

Koetz, B., Baret, F., Poilvé, H., Hill, J., 2005. Use of coupled canopy structure dynamic and radiative transfer models to estimate biophysical canopy characteristics. Remote Sens. Environ. 95, 115–124, http://dx.doi.org/10.1016/j.rse.2004.11.017

Lauvernet, C., Baret, F., Hascoët, L., Buis, S., Le Dimet, F.-X., 2008. Multitemporal-patch ensemble inversion of coupled surface – atmosphere radiative transfer models for land surface characterization. Remote Sens. Environ. 112, 851–861, http://dx.doi.org/10.1016/j.rse.2007.06.027

Lavergne T., Kaminski T., Pinty B., Taberner M., Gobron N., Verstraete M.M., Vossbeck M., Widlowski J.-L., Giering R., 2007. Application to MISR land products of an RPV model inversion package using adjoint and Hessian codes. Remote Sens. Environ., Multi-angle Imaging SpectroRadiometer (MISR) Special Issue MISR Special Issue 107, 362–375. doi:10.1016/j.rse.2006.05.021

Lee, K.-S., Cohen, W.B., Kennedy, R.E., Maiersperger, T.K., Gower, S.T., 2004. Hyperspectral versus multispectral data for estimating leaf area index in four different biomes. Remote Sens. Environ. 91, 508–520, http://dx.doi.org/10.1016/j.rse.2004.04.010

Le Maire, G., François, C., Soudani, K., Berveiller, D., Pontailler, J.-Y., Bréda, N., Genet, H., Davi, H., Dufrêne, E., 2008. Calibration and validation of hyperspectral indices for the estimation of broadleaved forest leaf chlorophyll content, leaf mass per area, leaf area index and leaf canopy biomass. Remote Sens. Environ. 112, 3846–3864, http://dx.doi.org/10.1016/j.rse.2008.06.005

Le Maire, G., Marsden, C., Nouvellon, Y., Stape, J.-L., Ponzoni, F.J., 2012. Calibration of a species-specific spectral vegetation index for leaf area index (LAI) monitoring: example with modis reflectance time-series on eucalyptus plantations. Remote Sens. 4, 3766–3780, http://dx.doi.org/10.3390/rs4123766

Le Maire, G., Marsden, C., Verhoef, W., Ponzoni, F.J., Lo Seen, D., Bégué, A., Stape, J.-L., Nouvellon, Y., 2011. Leaf area index estimation with MODIS reflectance time series and model inversion during full rotations of Eucalyptus plantations. Remote Sens. Environ. 115, 586–599, http://dx.doi.org/10.1016/j.rse.2010.10.004

Markwell, J., Osterman, J.C., Mitchell, J.L., 1995. Calibration of the minolta SPAD-502 leaf chlorophyll meter. Photosynth. Res. 46, 467–472, http://dx.doi.org/10.1007/BF00032301

McRoberts, R.E., Tomppo, E.O., Finley, A.O., Heikkinen, J., 2007. Estimating areal means and variances of forest attributes using the k-nearest neighbors technique and satellite imagery. Remote Sens. Environ. 111, 466–480, http://dx.doi.org/10.1016/j.rse.2007.04.002

Meroni, M., Colombo, R., Panigada, C., 2004. Inversion of a radiative transfer model with hyperspectral observations for LAI mapping in poplar plantations. Remote Sens. Environ. 92, 195–206, http://dx.doi.org/10.1016/j.rse.2004.06.005

Minolta, 2003. Chlorophyll meter SPAD-502. Instruction Manual, Minolta Camera BeNeLux BV. Maarssen, NL.

Mirzaie, M., Darvishzadeh, R., Shakiba, A., Matkan, A.A., Atzberger, C., Skidmore, A., 2014. Comparative analysis of different uni- and multi-variate methods for estimation of vegetation water content using hyper-spectral measurements.

Int. J. Appl. Earth Obs. Geoinf. 26, 1–11, http://dx.doi.org/10.1016/j.jag.2013.04.004

Mutanga, O., Skidmore, A.K., 2004. Narrow band vegetation indices overcome the saturation problem in biomass estimation. Int. J. Remote Sens. 25, 3999–4014, http://dx.doi.org/10.1080/01431160310001654923

Pereira, H.M., Ferrier, S., Walters, M., Geller, G.N., Jongman, R.H.G., Scholes, R.J., Bruford, M.W., Brummitt, N., Butchart, S.H.M., Cardoso, A.C., Coops, N.C., Dulloo, E., Faith, D.P., Freyhof, J., Gregory, R.D., Heip, C., Höft, R., Hurtt, G., Jetz, W., Karp, D.S., McGeoch, M.A., Obura, D., Onoda, Y., Pettorelli, N., Reyers, B., Sayre, R., Scharlemann, J.P.W., Stuart, S.N., Turak, E., Walpole, M., Wegmann, M., 2013. Essential biodiversity variables. Science 339, 277–278, http://dx.doi.org/10.1126/science.1229931

Pu, R., Gong, P., Biging, G.S., Larrieu, M.R., 2003. Extraction of red edge optical parameters from hyperion data for estimation of forest leaf area index. IEEE Trans. Geosci. Remote Sens. 41, 916–921, http://dx.doi.org/10.1109/TGRS.2003.813555

Richter, K., Atzberger, C., Vuolo, F., Weihs, P., D'Urso, G., 2009. Experimental assessment of the sentinel-2 band setting for RTM-based LAI retrieval of sugar beet and maize. Can. J. Remote Sens. 35, 230–247, http://dx.doi.org/10.5589/m09-010

Richter, R., Schläpfer, D., Müller, A., 2011. Operational atmospheric correction for imaging spectrometers accounting for the smile effect. IEEE Trans. Geosci. Remote Sens. 49, 1772–1780, http://dx.doi.org/10.1109/TGRS2010.2089799

Rivera, J.P., Verrelst, J., Delegido, J., Veroustraete, F., Moreno, J., 2014a. On the semi-automatic retrieval of biophysical parameters based on spectral index optimization. Remote Sens. 6, 4927–4951, http://dx.doi.org/10.3390/rs6064927

Rivera, J.P., Verrelst, J., Leonenko, G., Moreno, J., 2013. Multiple cost functions and regularization options for improved retrieval of leaf chlorophyll content and LAI through inversion of the PROSAIL model. Remote Sens. 5, 3280–3304, http://dx.doi.org/10.3390/rs5073280

Rivera, J.P., Verrelst, J., Munoz-Mari, J., Moreno, J., Camps-Valls, G., 2014b. Toward a semiautomatic machine learning retrieval of biophysical parameters. IEEE J. Sel. Top. Appl. Earth Obs. Remote Sens. 7, 1249–1259, http://dx.doi.org/10.1109/JSTARS.2014.2298752

Röder, A., Kuemmerle, T., Hill, J., Papanastasis, V.P., Tsiourlis, G.M., 2007. Adaptation of a grazing gradient concept to heterogeneous Mediterranean rangelands using cost surface modelling. Ecol. Model. 204, 387–398, http://dx.doi.org/10.1016/j.ecolmodel.2007.01.022

Schaepman, M.E., Ustin, S.L., Plaza, A.J., Painter, T.H., Verrelst, J., Liang, S., 2009. Earth system science related imaging spectroscopy—an assessment. Remote Sens. Environ. 113, 123–137, http://dx.doi.org/10.1016/j.rse.2009.03.001, Imaging Spectroscopy Special Issue.

Schlerf, M., Atzberger, C., 2006. Inversion of a forest reflectance model to estimate structural canopy variables from hyperspectral remote sensing data. Remote Sens. Environ. 100, 281–294, http://dx.doi.org/10.1016/j.rse.2005.10.006

Schlerf, M., Atzberger, C., Hill, J., Buddenbaum, H., Werner, W., Schüler, G., 2010. Retrieval of chlorophyll and nitrogen in Norway spruce (*Picea abies* L. Karst.) using imaging spectroscopy. Int. J. Appl. Earth Obs. Geoinfn. 12, 17–26, http://dx.doi.org/10.1016/j.jag.2009.08.006

Segl, K., Guanter, L., Kaufmann, H., Schubert, J., Kaiser, S., Sang, B., Hofer, S., 2010. Simulation of spatial sensor characteristics in the context of the enmap hyperspectral mission. IEEE Trans. Geosci Remote Sens. 48, 3046–3054, http://dx.doi.org/10.1109/TGRS2010.2042455

Si, Y., Schlerf, M., Zurita-Milla, R., Skidmore, A., Wang, T., 2012. Mapping spatio-temporal variation of grassland quantity and quality using MERIS data and the PROSAIL model. Remote Sens. Environ. 121, 415–425, http://dx.doi.org/10.1016/j.rse.2012.02.011

Thenkabail, P.S., Smith, R.B., De Pauw, E., 2000. Hyperspectral vegetation indices and their relationships with agricultural crop characteristics. Remote Sens. Environ. 71, 158–182, http://dx.doi.org/10.1016/S0034-4257(99)00067-X

Turner, D.P., Cohen, W.B., Kennedy, R.E., Fassnacht, K.S., Briggs, J.M., 1999. Relationships between leaf area index and landsat TM spectral vegetation indices across three temperate zone sites. Remote Sens. Environ. 70, 52–68, http://dx.doi.org/10.1016/S0034-4257(99)00057-7

Verger, A., Baret, F., Camacho, F., 2011. Optimal modalities for radiative transfer-neural network estimation of canopy biophysical characteristics: evaluation over an agricultural area with CHRIS/PROBA observations. Remote Sens. Environ. 115, 415–426, http://dx.doi.org/10.1016/j.rse.2010.09.012

Verhoef, W., 1984. Light scattering by leaf layers with application to canopy reflectance modeling: the SAIL model. Remote Sens. Environ. 16, 125–141, http://dx.doi.org/10.1016/0034-4257(84)90057-9

Vohland, M., Jarmer, T., 2008. Estimating structural and biochemical parameters for grassland from spectroradiometer data by radiative transfer modelling (PROSPECT + SAIL). Int. J. Remote Sens. 29, 191–209, http://dx.doi.org/10.1080/01431160701268947

Vuolo, F., Neugebauer, N., Bolognesi, S.F., Atzberger, C., D'Urso, G., 2013. Estimation of leaf area index using DEIMOS-1 data: application and transferability of a semi-empirical relationship between two agricultural areas. Remote Sens. 5, 1274–1291, http://dx.doi.org/10.3390/rs5031274

Weiss, M., Baret, F., 1999. Evaluation of canopy biophysical variable retrieval performances from the accumulation of large swath satellite data. Remote Sens. Environ. 70, 293–306, http://dx.doi.org/10.1016/S0034-4257(99)00045-0

Weiss, M., Baret, F., Myneni, R., Pragnère, A., Knyazikhin, Y., 2000. Investigation of a model inversion technique to estimate canopy biophysical variables from spectral and directional reflectance data. Agronomie 20, 3–22, http://dx.doi.org/10.1051/agro:2000105

Welles, J.M., Norman, J.M., 1991. Instrument for Indirect measurement of canopy architecture. Agron. J. 83, 818, http://dx.doi.org/10.2134/agronj1991.00021962008300050009x

Yang, G., Zhao, C., Liu, Q., Huang, W., Wang, J., 2011. Inversion of a radiative transfer model for estimating forest LAI from multisource and multiangular optical remote sensing data. IEEE Trans. Geosci. Remote Sens. 49, 988–1000, http://dx.doi.org/10.1109/TGRS2010.2071416

Yu, K., Li, F., Gnyp, M.L., Miao, Y., Bareth, G., Chen, X., 2013. Remotely detecting canopy nitrogen concentration and uptake of paddy rice in the Northeast China Plain. ISPRS J. Photogramm Remote Sens. 78, 102–115, http://dx.doi.org/10.1016/j.isprsjprs.2013.01.008

Zhao, K., Valle, D., Popescu, S., Zhang, X., Mallick, B., 2013. Hyperspectral remote sensing of plant biochemistry using Bayesian model averaging with variable and band selection. Remote Sens. Environ. 132, 102–119, http://dx.doi.org/10.1016/j.rse.2012.12.026.